

Article

# Identification and Expression Analysis of Two *allene oxide cyclase* (AOC) Genes in Watermelon

Jingwen Li <sup>1,2</sup>, Yelan Guang <sup>1,2</sup>, Youxin Yang <sup>1,2,\*</sup> and Yong Zhou <sup>2,3,\*</sup> 

<sup>1</sup> Jiangxi Key Laboratory for Postharvest Technology and Nondestructive Testing of Fruits & Vegetables, Collaborative Innovation Center of Post-Harvest Key Technology and Quality Safety of Fruits and Vegetables, College of Agronomy, Jiangxi Agricultural University, Nanchang 330045, China; 18770911287@163.com (J.L.); 15357167302@163.com (Y.G.)

<sup>2</sup> Key Laboratory of Crop Physiology, Ecology and Genetic Breeding, Ministry of Education, Jiangxi Agricultural University, Nanchang 330045, China

<sup>3</sup> Jiangxi Engineering Laboratory for the Development and Utilization of Agricultural Microbial Resources, College of Bioscience and Bioengineering, Jiangxi Agricultural University, Nanchang 330045, China

\* Correspondence: yangyouxin@jxau.edu.cn (Y.Y.); yongzhou@jxau.edu.cn (Y.Z.)

Received: 2 August 2019; Accepted: 14 October 2019; Published: 17 October 2019



**Abstract:** Allene oxide cyclase (AOC, EC 5.3.99.6) catalyzes the most important step in the jasmonic acid (JA) biosynthetic pathway and mediates plant defense response to a wide range of biotic and abiotic stresses. In this study, two AOC genes were identified from watermelon. Sequence analysis revealed that each of *CIAOC1* and *CIAOC2* contained an allene oxide cyclase domain and comprised eight highly conserved  $\beta$ -strands, which are the typical characteristics of AOC proteins. Phylogenetic analysis showed that *CIAOC1* and *CIAOC2* were clustered together with AOCs from dicotyledon, with the closest relationships with *JcAOC* from *Jatropha curcas* and *Ljaoc1* from *Lotus japonicus*. Different intron numbers were observed in *CIAOC1* and *CIAOC2*, which may result in their functional divergence. qRT-PCR analysis revealed that *CIAOC1* and *CIAOC2* have specific and complex expression patterns in multiple organs and under hormone treatments. Both *CIAOC1* and *CIAOC2* displayed the highest transcriptional levels in stem apex and fruit and exhibited relatively lower expression in stem. JA, salicylic acid (SA), and ethylene (ET) could enhance the expression of *CIAOC1* and *CIAOC2*, particularly that of *CIAOC2*. Red light could induce the expression of *CIAOC2* in root-knot nematode infected leaf and root of watermelon, indicating that *CIAOC2* might play a primary role in red light-induced resistance against root-knot nematodes through JA signal pathway. These findings provide important information for further research on AOC genes in watermelon.

**Keywords:** watermelon; allene oxide cyclase (AOC); jasmonic acid (JA); expression profile; root-knot nematode

## 1. Introduction

Jasmonates, including jasmonic acid (JA) and its related compounds, play vital roles in plant developmental processes and responses to various biotic and abiotic stresses [1,2]. Jasmonate is biosynthesized from  $\alpha$ -linolenic acid through a canonical pathway, and allene oxide cyclase (AOC, EC 5.3.99.6) is one of the most important enzymes, which produces 12-oxo-phytodienoic acid (OPDA) with 12,13(S)-epoxy-octadecatrienoic acid (12,13-EOT), and establishes the stereochemical configuration of naturally occurring JA [3–6].

Several studies have shown that AOC genes compose a small gene family, and the numbers of AOC genes are different across plants. For example, there are six AOC genes in soybean [7], five in upland cotton (*Gossypium hirsutum*) [8], four in *Arabidopsis thaliana* [9], three in *Lotus japonicus* [10], two in *Physcomitrella patens* [11], while only one AOC gene in rice and tomato [6,12], respectively. In addition,

AOC genes were found to have specific and complicated tissue expression patterns in different plants. In barley, *HvAOC* mRNA accumulation is abundant in root tip, scutellar node, and leaf base [13]. Soybean *GmAOC1* and *GmAOC2* also exhibited abundant mRNA transcripts in roots, while *GmAOC3* and *GmAOC4* showed relatively higher expression in leaves and stems, respectively [7]. *Camptotheca acuminata* *CaAOC* is constitutively expressed in various organs, with the highest expression level in leaves [14]. In *Arabidopsis*, *AtAOC1*, *AtAOC2*, and *AtAOC3* promoters exhibit high activities in the leaves, while only *AtAOC3* and *AtAOC4* show promoter activity in roots [15]. These results suggest that AOC genes are involved in the regulation of multiple plant developmental processes.

The expression of jasmonate biosynthetic pathway genes, including AOCs, is regulated by JA, and overexpression or suppression of these genes can greatly affect the JA levels in plants. For example, a severe deficiency of jasmonate was found in two AOC mutants (*cpm2* and *hebiba*) of rice [12], and partial suppression of *MtAOC1* in hairy roots of *Medicago truncatula* also resulted in lower JA levels in mycorrhizal roots [16]. In addition, elevated JA levels were found in transgenic plants overexpressing AOC genes from different plants, such as *AaAOC* from *Artemisia annua* [5], *TaAOC1* from wheat [17], and *GmAOC3* from soybean [18]. JA and its related compounds are involved in plant defense reactions against biotic and abiotic stresses, and the expression of some AOC genes can also be regulated by various stresses, implying that they may play regulatory roles in response to abiotic and biotic stresses. For example, overexpression of *GmAOC1* and *GmAOC5* in transgenic tobacco plants contributed to significantly increased resistance to salinity and oxidative stress, respectively [7], whereas *GmAOC3* confers resistance to common cutworm (CCW) in transgenic tobacco plants [18]. Rice AOC mutants were less sensitive to salt stress but susceptible to *Magnaporthe oryzae*, and exogenous application of JA restored the resistance to *M. oryzae* in these mutants [12,19], while overexpression of *OsAOC* in rice significantly increased the resistance to chewing and piercing-sucking insect pests through AOC-mediated increases of OPDA and JA, respectively [20]. Overexpression of peanut *AhAOC* in rice resulted in increases of root elongation and plant height and improved salt tolerance with increased expression of stress-responsive genes [21]. Overexpression of *Cymbidium faberi* *CfAOC* gene in tomato also resulted in significantly enhanced drought tolerance with increased expression levels of genes related to MeJA biosynthesis [22].

Watermelon is an important agricultural crop and can be invaded by root-knot nematode (RKN) *Meloidogyne incognita*, which finally causes substantial losses of crop production [23]. Various hormones, such as JA, salicylic acid (SA), and ethylene (ET), are key components in plant defense against nematode infection, and red light (RL) could potentially activate systemic defense against RKN by modulating hormone pathways [23–26]. A previous study has shown that loss-of-function of *AtAOC3* rendered plants are more susceptible to nematode infection [27], suggesting that AOC genes may be involved in plant defense against RKN. However, less information is available about the AOC genes in watermelon. In the present study, two AOC genes were identified from watermelon, and their phylogenetic relationships, gene structures, expression profiles in response to JA, SA, ET, red light, and RKN were also examined. The findings provide further insights into the role of AOC genes in watermelon.

## 2. Materials and Methods

### 2.1. Identification and Sequence Analysis of the AOC Genes in Watermelon

To identify the AOC members in watermelon and other plants, watermelon genomic database (<http://cucurbitgenomics.org/search/genome/1>) and plant genomic resource Phytozome (<https://phytozome.jgi.doe.gov/pz/portal.html>) were screened using AOC protein sequences of in tomato, rice, and *Arabidopsis* as queries. The possible AOC proteins were confirmed with NCBI CDD program (<https://www.ncbi.nlm.nih.gov/Structure/cdd/wrpsb.cgi>). The physicochemical properties including isoelectric point (pI), molecular weight (MW), and grand average of hydropathy index (GRAVY) of the AOC proteins were analyzed by using the ProtParam tool (<http://web.expasy.org/protparam/>). GSDS (Gene Structure Display Server) tool was employed to analyze the gene structures of AOC family

genes from different plant species by comparing the coding sequences (CDSs) and the genomic DNA (gDNA) sequences.

### 2.2. Alignment of Amino Acid Sequences and Phylogenetic Analysis

For multiple sequence alignment, the full-length AOC protein sequences from watermelon and other plant species in literature were aligned using Clustal Omega with default settings and visualized with GeneDoc [28]. To investigate the evolutionary relationships of AOC genes among different plant species, a phylogenetic tree was created with the MEGA 7.0 software program by using the neighbor-joining (NJ) method with bootstrap analysis of 1000 replicates.

### 2.3. Expression Pattern Analysis of the AOC Genes in Different Tissues

For analysis of the expression of watermelon AOC genes during the fruit development, the transcriptome data of both the rind and flesh at different stages of fruit development were obtained based on a previous study [29]. The transcriptome data were analyzed and the expression was picked out and displayed as fragments per kilobase of exon model per million mapped (FPKM) values as previously described [24,28].

### 2.4. Plant Materials and Growth Conditions

Watermelon (*Citrullus lanatus* L. cv. Xinong 8) seeds were germinated and sown in pots containing nutritional soil, placed in greenhouse under the conditions of 25 °C/19 °C (12 h/12 h), and light intensity of 200  $\mu\text{mol}\cdot\text{m}^{-2}\cdot\text{s}^{-1}$ . Seedlings at 2-month-old stage were harvested for tissues including the leaves, stems, stem apices, fruits, flowers, and roots. For hormonal stresses, the leaves or roots of the four-leaf stage watermelon seedlings were used to test the expression levels of *CIAOC1* and *CIAOC2* using qRT-PCR at different time points (0, 1, 3, 9, and 24 h) with 100  $\mu\text{M}$  methyl jasmonate (MeJA), 1 mM salicylic acid (SA), and 500  $\mu\text{M}$  ethylene (ET) spraying on watermelon leaves, respectively. For analysis of the expression of watermelon AOC genes in response to red light induction of watermelon against root-knot nematode infection, the experiment was conducted according to our previous study [23], and the samples of leaves and roots from control (mock, white light, and water solution), RL (red light treatment and water solution), RKN (white light and root knot nematode *M. incognita* infection), and RR (red light treatment and root knot nematode *M. incognita* infection) treatments were collected. All samples were immediately frozen in liquid nitrogen and stored at  $-80$  °C for RNA extraction.

### 2.5. RNA Isolation, cDNA Synthesis, and Quantitative Real-Time PCR of the AOC Genes in Watermelon

Total RNA was extracted with the total RNA Miniprep Kit (Axygen Biosciences, Union City, CA, USA), and reverse transcribed using the ReverTra Ace qPCR-RT Kit (Toyobo, Japan) according to the manufacturers' protocols. qRT-PCR was carried out using the iCycler iQTM Real-time PCR Detection System (Bio-Rad, Hercules, CA, USA) in three replicates with the procedure as follows: 3 min at 95 °C, followed by 40 cycles of 30 s at 95 °C, 30 s at 58 °C and 1 min at 72 °C. Watermelon  $\beta$ -actin gene (Cla007792) was used as an internal control, and qRT-PCR data were compared with those of 0 h and the relative expression values were calculated using the method described previously [30]. Significant differences ( $p < 0.05$ ) were determined with Tukey's test in the SPSS software, and the differences were indicated by different letters.

## 3. Results and Discussion

### 3.1. Identification and Sequence Analysis of the AOC Genes in Watermelon

Two AOC genes, Cla016453 and Cla003512, were identified in watermelon genome and were named as *CIAOC1* and *CIAOC2*, respectively. The *CIAOC1* coding sequence (CDS) consisted of 741 nucleotides and encoded a putative protein of 246 amino acids, with a predicted isoelectric point (pI) of 8.74 and a molecular weight (MW) of 28.86 kDa (Table 1). The *CIAOC2* gene contained a 1005-bp

CDS, which encoded a putative protein of 334 amino acids, with a predicted pI of 9.62 and a MW of 36.67 kDa. The predicted GRAVY values of *CIAOC1* and *CIAOC2* were  $-0.268$  and  $-0.309$ , respectively (Table 1), suggesting that both of them are hydrophilic. Domain analyses by CDD showed that each of *CIAOC1* and *CIAOC2* contained an allene oxide cyclase domain (Figure 1), which was located on their C-terminus, indicating that they are members of the AOC gene family.

**Table 1.** The basic characterizations of *CIAOC* genes in watermelon.

Gene	Gene ID	Genomic Position	gDNA (bp)	ORF (bp)	Length (aa)	pI	MW (kDa)	GRAVY
<i>CIAOC1</i>	Cla016453	Chr11: 21540468 .. 21542845 (+)	2378	741	246	8.74	28.86	$-0.268$
<i>CIAOC2</i>	Cla003512	Chr3: 13175215 .. 13176809 (+)	1595	1005	334	9.62	36.67	$-0.309$

gDNA, genomic DNA; bp, base pair; ORF, open reading frame; aa, amino acid; MW, molecular weight; pI, isoelectric point; GRAVY, grand average of hydropathicity.



**Figure 1.** Domain analyses of the putative *CIAOC1* and *CIAOC2* proteins.

### 3.2. Characterization of *CIAOC1* and *CIAOC2*

To characterize *CIAOC1* and *CIAOC2*, a multiple sequence alignment was performed for their full-length amino acid sequences, as well as other published AOC proteins, such as SIAOC from *Solanum lycopersicum* [6], HvAOC from *Hordeum vulgare* [13], HnAOC from *Hyoscyamus niger* [31], JcAOC from *Jatropha curcas* [32], AaAOC from *Artemisia annua* [33], OsAOC from *Oryza sativa* [12], LmAOC from *Leymus mollis* [34], TaAOC1 from *Triticum aestivum* [17], GhAOC1 from *Gossypium hirsutum* [8], GmAOC3 from *Glycine max* [18], CsAOC from *Camellia sinensis* [35], and Ljaoc1 from *Lotus japonicus* [10]. The results showed that the identity between *CIAOC1* and *CIAOC2* was 62.13%, and the amino acid sequences of *CIAOC1* and *CIAOC2* shared 58.05% to 69.08% identity with other AOC proteins (Figure 2). It should be noted that all of these AOC proteins comprised eight highly conserved  $\beta$ -strands (Figure 2), which might play vital roles in determining the biological function of the AOC enzymes [7,36,37]. Therefore, *CIAOC1* and *CIAOC2* might have similar functions with their homologs in other plant species.

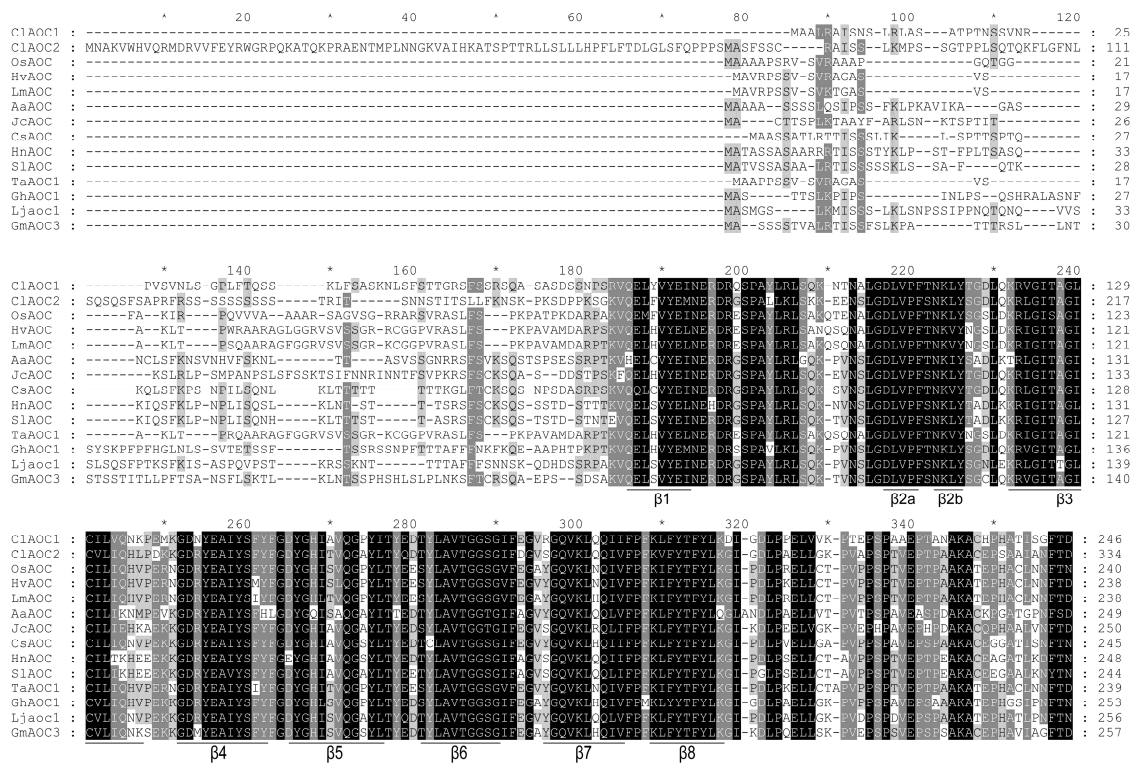


**Figure 2.** Alignment of the deduced amino acid sequence of *CIAOC1* and *CIAOC2* with other AOC proteins from different plant species. The eight  $\beta$ -strands are underlined. The accession numbers of AOC proteins are as follows: JcAOC, ACZ06580.1; OsAOC, ABV45432.1; HnAOC, AAU11327.1; AaAOC, ADL16493.1; SIAOC, CAC83760; TaAOC1, AHA93095.1; GHAOC1, ALG62635.1; LmAOC, AFP87304.1; CsAOC, ADY38579.1; GmAOC3, AEE99198.1; HvAOC, CAC83766.1; Ljaoc1, AB600747.1.

### 3.3. Phylogenetic and Structural Analyses of AOC Genes from Different Plant Species

To investigate the evolutionary relationships of AOC genes within multiple plant species, a phylogenetic tree was created by MEGA 7.0 with the NJ method by using the full-length amino acid sequences of AOC proteins from different plant species. As a result, these AOC proteins were found to originate from a common ancestor and could be divided into three groups (Figure 3). *CIAOC1* and *CIAOC2* clustered together with AOCs from dicotyledon in Group I, which is in accordance with the category of watermelon. Amongst them, *CIAOC1* and *CIAOC2* showed the closest relationships with JcAOC and Ljaoc1, respectively (Figure 3). In addition, the monocotyledonous AOCs from rice, *L. mollis*, wheat, barley, maize, and sorghum were clustered together in Group II. Four AtAOC proteins together with GHAOC1 were clustered in Group III and diverged earlier than other species (Figure 3), which is consistent with the previous reports [9,33].

The gene structures can provide important information to reveal the evolutionary relationships among gene families [30]. We then performed the structural analyses of AOC family genes from watermelon and other plant species such as *Arabidopsis*, rice, tomato, maize, and sorghum. It should be noted that tomato, sorghum, and rice contain a single AOC gene. Most AOC genes contained two exons and one intron, while *SIAOC* and *CIAOC1* possessed three exons and two introns (Figure 4). The members with close phylogenetic relationships shared similar gene structures, including intron numbers and CDS lengths, revealing the conserved features during the evolution of AOC genes. It is noteworthy that *CIAOC1* and *CIAOC2* harbored different numbers of introns, which may result in their functional divergence. Similarly, four soybean AOC genes (*GmAOC3-6*) have two introns, and other two AOC genes (*GmAOC1* and *GmAOC2*) contain only one intron [7].

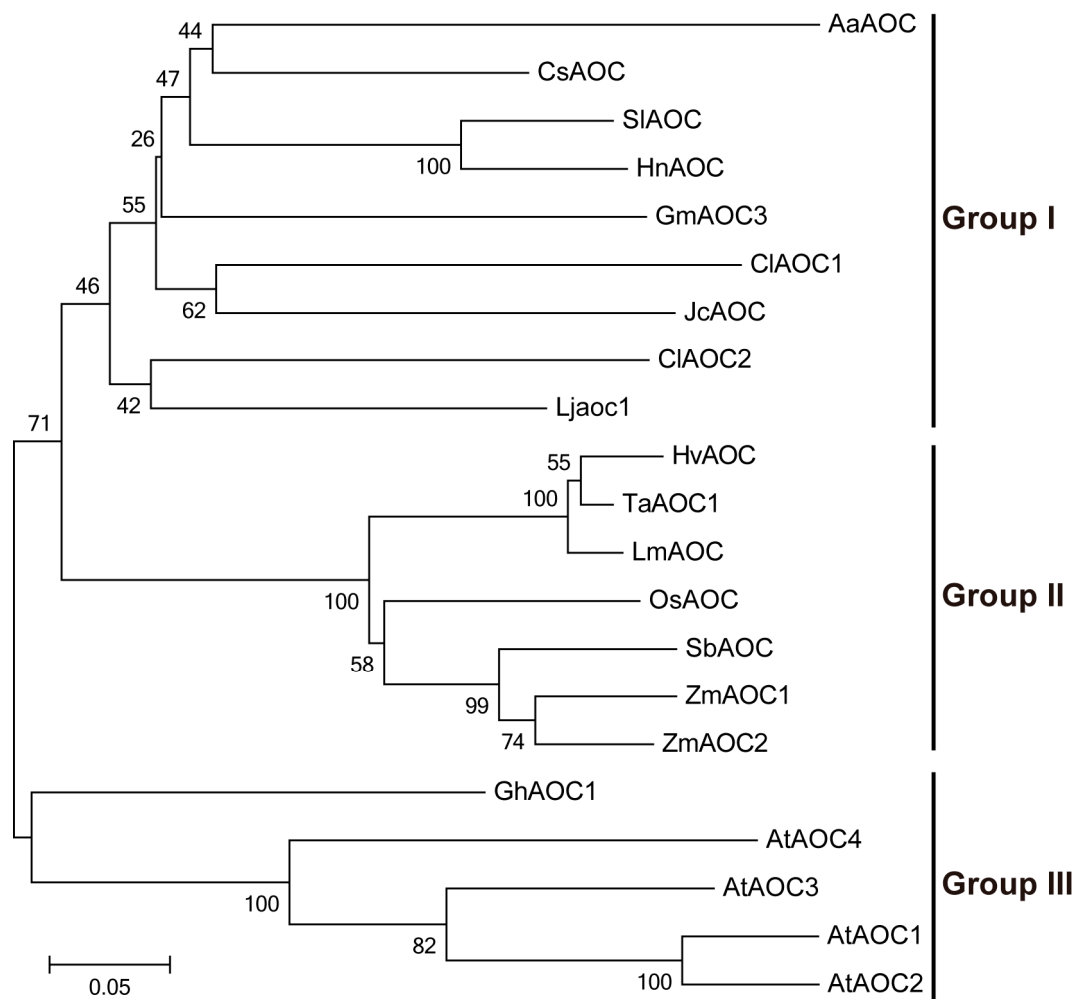


**Figure 3.** Phylogenetic analysis of AOC proteins from different plant species. The phylogenetic tree was created by MEGA 7.0 using the NJ method based on full-length amino acid sequences of AOC proteins from different plant species. The bootstrap value was set to 1000 replicates. The protein IDs and sources of all AOC proteins are listed in Table S2.

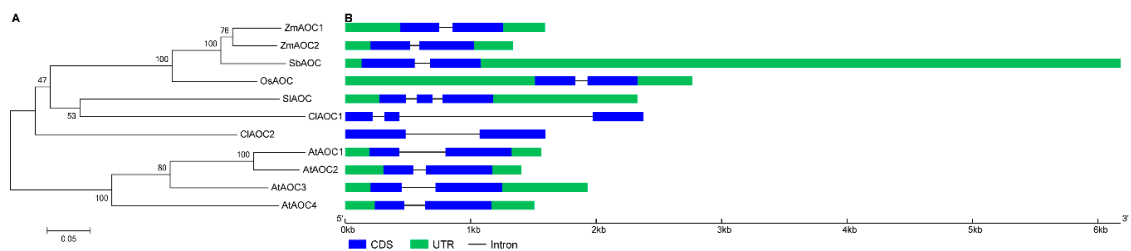


**Figure 4.** The gene structures of AOC family genes from different plant species (B) based on the phylogenetic relationship (A). The green boxes, blue boxes, and black lines indicate UTRs, CDSs, and introns, respectively.

### 3.4. Expression Patterns of CIAOC1 and CIAOC2 in Different Tissues

The expression patterns of *CIAOC1* and *CIAOC2* in different tissues were determined by qRT-PCR. Both *CIAOC1* and *CIAOC2* displayed the high transcriptional levels in stem apex and the lowest expression levels in stem (Figure 5). In addition, their expression was also detected in flower and fruit at relatively high levels. It is noteworthy that *CIAOC1* displayed higher transcriptional levels in fruit than in flower, while *CIAOC2* exhibited higher transcriptional levels in flower than in

fruit (Figure 5). In *Arabidopsis*, *AtAOC1* and *AtAOC4* promoters were found to be active in flower development [15]. To further access the functions of the *CIAOC1* and *CIAOC2* in the developmental regulation, their expression during the development of flesh and rind at different stages was examined. According to the transcriptome data, *CIAOC1* showed much higher expression during fruit development than *CIAOC2* (Figure 6). Both *CIAOC1* and *CIAOC2* displayed gradually declining expression during the earlier development of flesh, while their expression increased at 34 DAP. During the rind development, the expression of *CIAOC1* increased gradually, while that of *CIAOC2* exhibited a down-regulated trend (Figure 6). These results suggested that *CIAOC1* and *CIAOC2* play different roles in the fruit development of watermelon.

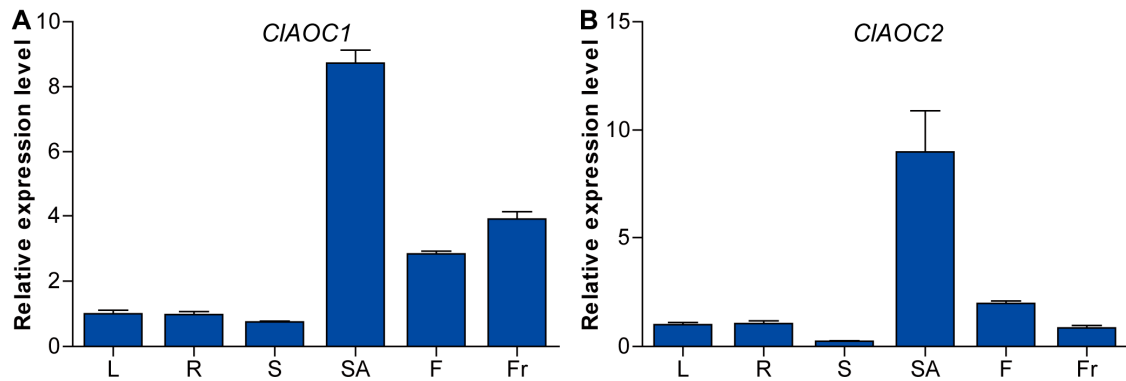


**Figure 5.** Relative mRNA levels of *CIAOC1* (A) and *CIAOC2* (B) determined by qRT-PCR in different tissues of watermelon. The  $\beta$ -actin gene was used as the internal control to standardize for each reaction. L, leaf; R, root; S, stem; SA, stem apex; F, flower; Fr, fruit.

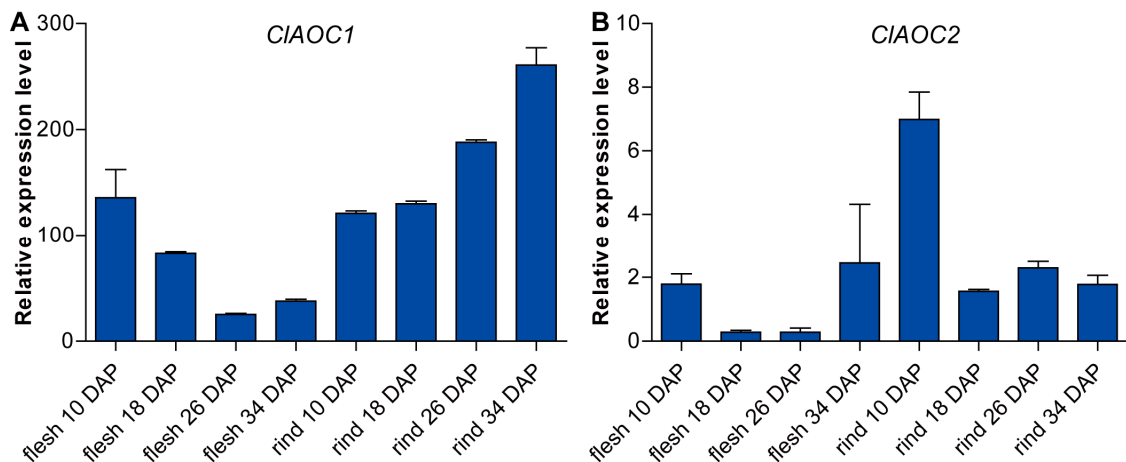


**Figure 6.** The expression of *CIAOC1* (A) and *CIAOC2* (B) during the development of flesh and rind at different stages based on the transcriptome data. The expression levels were indicated FPKM values. DAP, day after pollination.

### 3.5. Expression Patterns of *CIAOC1* and *CIAOC2* in Response to Hormones

Previous studies have revealed that the expression of *AOC* genes could be induced by treatments of different hormones, such as JA and SA [8,35,37]. To determine whether *CIAOC1* and *CIAOC2* are responsive to hormones, their expression patterns under treatments of different hormones (JA, SA, and ET) were examined by qRT-PCR. The results showed that the two genes displayed markedly up-regulated expression in response to these hormones. Upon JA treatment, the transcription levels of *CIAOC1* and *CIAOC2* were significantly up-regulated at 1 h and 3 h both in leaf and root, and their expression levels showed a decline trend at 9 h and 24 h (Figure 7A,B). The expression pattern was similar to that of *AOC* genes in *Salvia miltiorrhiza* [37] and *G. hirsutum* [8]. However, the expression

of *CIAOC1* and *CIAOC2* was increased to different degrees in leaf and root. In leaf, the rising trend of *CIAOC1* was more rapid than in root, while that of *CIAOC2* was just the opposite (Figure 7A,B), implying that these two genes have different roles for JA signaling in leaf and root. For SA and ET treatments, the transcription levels of *CIAOC1* and *CIAOC2* increased gradually at the earlier stage but showed significant decreases at the later stage (Figure 7C,D). The expression of *CIAOC1* peaked at 9 h and 3 h under SA and ET treatment, respectively. However, the expression of *CIAOC2* reached the maximum at 1 h and then gradually decreased under SA and ET treatments (Figure 7C,D). Similarly, the expression of *CsAOC* also increased rapidly at the earlier time points after SA treatment and then decreased gradually [35]. In particular, the highest mRNA accumulation of *CIAOC2* was observed after 3 h of JA treatment in root, which was significantly higher than that of control and under treatments with other hormones (Figure 7). The results indicated that *CIAOC1* and *CIAOC2* might play vital and diverse roles in hormone responses.

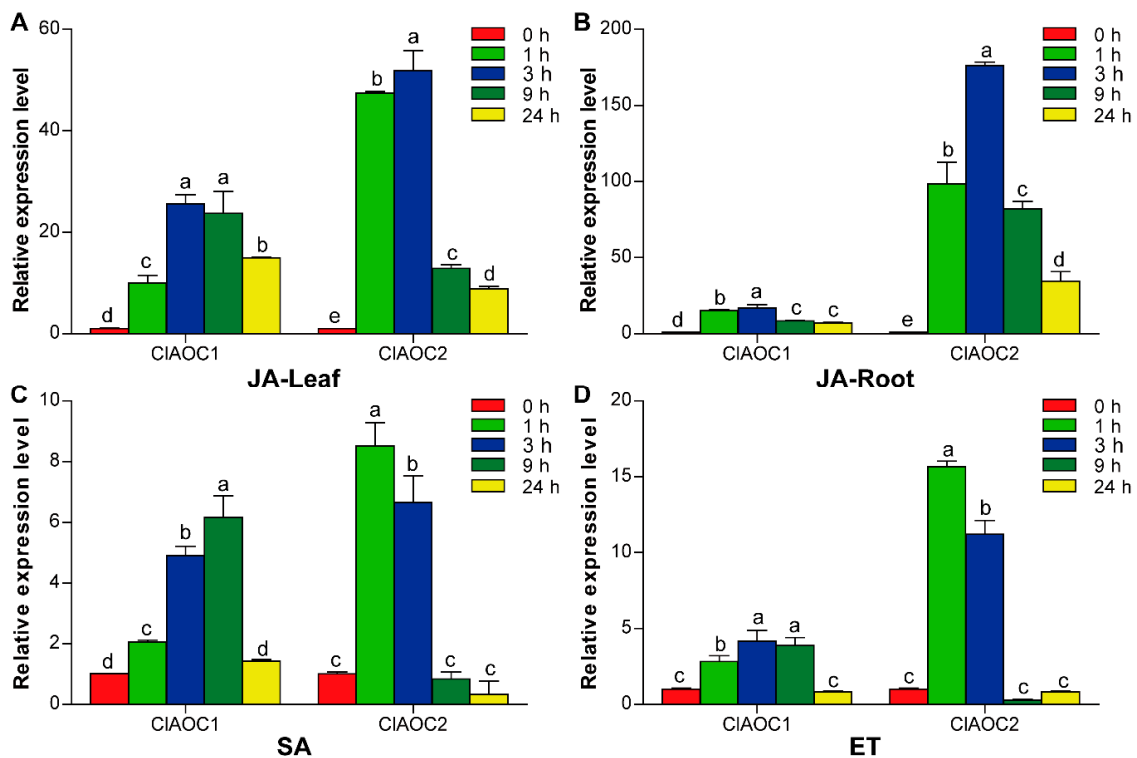


**Figure 7.** qRT-PCR analysis of *CIAOC1* and *CIAOC2* under different hormones treatments, including JA (A,B), SA (C), and ET (D). The leaves (A,C,D) or roots (B) of the watermelon seedlings were used to examine the expression levels of *CIAOC1* and *CIAOC2* using qRT-PCR at different time points (0, 1, 3, 9, and 24 h) with different hormones treatments.

### 3.6. Expression Patterns of *CIAOC1* and *CIAOC2* in Response to Root-Knot Nematode Infection

Previous studies have revealed that red light (RL) could stimulate JA and SA biosynthesis and signaling pathway genes to activate plant defense against RKN [23,24]. Considering that *CIAOC1* and *CIAOC2* were induced by JA and SA, they may play a role in watermelon defense against RKN. To verify this speculation, we examined the expression of *CIAOC1* and *CIAOC2* in the leaves and roots under the treatments of CK, RKN, RL, and RR by qRT-PCR based on the experiment procedures in our previous study [23]. There was no significant difference in the expression of *CIAOC1* and *CIAOC2* under RKN treatment compared with the control (CK) in leaf (Figure 8A). However, the expression levels of *CIAOC1* and *CIAOC2* were obviously increased not only under RL treatment compared with CK but also under RR treatment compared with RKN treatment (Figure 8A). In root, only *CIAOC2* was observably up-regulated not only by RL treatment compared with CK but also by RR treatment

compared with RKN treatment (Figure 8B). In addition, the unequal rises of *CIAOC1* and *CIAOC2* in response to the treatments of CK, RKN, RL, and RR suggested that *CIAOC2* might play a primary role in red light-induced resistance against root-knot nematodes. AOC plays a vital role in JA biosynthesis, and this phytohormone can regulate plant defense against RKN [23,24,38]. Light can regulate plant defense by modifying multiple hormonal pathways including JA signaling and homeostasis [23,39,40]. After the induction of the generation of JA, it can be long-distance transported in plants through the vascular system [41–43]. Therefore, exposure of watermelon leaves to RL could influence the expression of *CIAOC1* and *CIAOC2* to produce JA in leaves, which can be transported to root and thus induce the expression of jasmonate biosynthetic genes to increase the JA content in root and finally induce watermelon resistance against RKN infection.

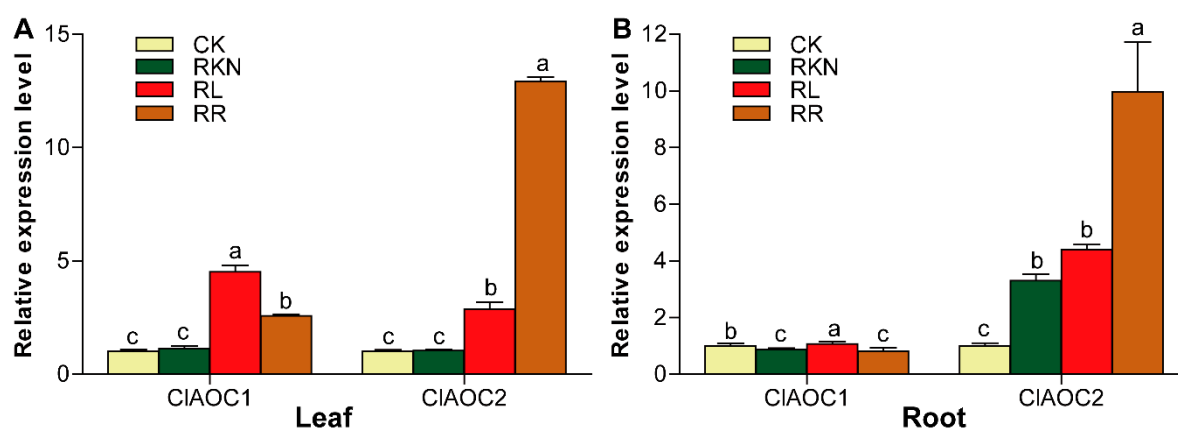


**Figure 8.** qRT-PCR analysis of expression of *CIAOC1* and *CIAOC2* in leaves (A) and roots (B) of inoculation with nematode under the treatments of white light (RKN), red light and water control (RL), nematode under red light (RR) and white light and clean water (CK).

#### 4. Conclusions

In this study, a systematic analysis of the AOC genes in watermelon was carried out through analysis of the protein structure, phylogenetic relationship, gene structure, and the expression profiles. Each of *CIAOC1* and *CIAOC2* contained an allene oxide cyclase domain and eight highly conserved  $\beta$ -strands, but *CIAOC1* and *CIAOC2* harbored different numbers of introns. In addition, the expression analysis revealed that *CIAOC1* and *CIAOC2* have distinct expression patterns in different tissues and in responses to hormones, implying that they may have different roles in the developmental regulation. Moreover, both of *CIAOC1* and *CIAOC2* were obviously induced not only under RL treatment compared with CK but also under RR treatment compared with RKN treatment in leaf. However, only *CIAOC2* was observably up-regulated not only by RL treatment compared with CK but also by RR treatment compared with RKN treatment in root. The different expression profiles of *CIAOC1* and *CIAOC2* indicate their diverse roles in the growth and development of watermelon.

**Supplementary Materials:** The following are available online at <http://www.mdpi.com/2077-0472/9/10/225/s1>, Table S1: Primers sequences used in qRT-PCR, Table S2: AOC proteins from different plant species used for phylogenetic analysis.

**Author Contributions:** Data curation, J.L., Y.G., Y.Y., and Y.Z.; formal analysis, J.L.; funding acquisition, Y.Y. and Y.Z.; methodology, Y.Y. and Y.Z.; resources, J.L., Y.G., and Y.Y.; software, Y.G. and Y.Z.; writing—original draft, Y.Z.; writing—review and editing, Y.Y. and Y.Z.

**Funding:** This research was funded by the Foundation of Jiangxi Educational Committee (GJJ160393 and GJJ180172), the National Natural Science Foundation of China (31560572), and the Natural Science Foundation of Jiangxi Province, China (20171BAB214030).

**Conflicts of Interest:** The authors declare that they have no conflict of interest.

## References

1. Lyons, R.; Manners, J.M.; Kazan, K. Jasmonate biosynthesis and signaling in monocots: A comparative overview. *Plant Cell Rep.* **2013**, *32*, 815–827. [[CrossRef](#)] [[PubMed](#)]
2. Per, T.S.; Khan, M.I.R.; Anjum, N.A.; Masood, A.; Hussain, S.J.; Khan, N.A. Jasmonates in plants under abiotic stresses: Crosstalk with other phytohormones matters. *Environ. Exp. Bot.* **2018**, *145*, 104–120. [[CrossRef](#)]
3. Stumpe, M.; Feussner, I. Formation of oxylipins by CYP74 enzymes. *Phytochem. Rev.* **2006**, *5*, 347–357. [[CrossRef](#)]
4. Hamberg, M.; Fahlstadius, P. Allene oxide cyclase: A new enzyme in plant lipid metabolism. *Arch. Biochem. Biophys.* **1990**, *276*, 518–526. [[CrossRef](#)]
5. Lu, X.; Zhang, F.; Shen, Q.; Jiang, W.; Pan, Q.; Lv, Z.; Yan, T.; Fu, X.; Wang, Y.; Qian, H.; et al. Overexpression of allene oxide cyclase improves the biosynthesis of artemisinin in *Artemisia annua* L. *PLoS ONE* **2014**, *9*, e91741. [[CrossRef](#)]
6. Ziegler, J.; Stenzel, I.; Hause, B.; Maucher, H.; Hamberg, M.; Grimm, R.; Ganai, M.; Wasternack, C. Molecular cloning of allene oxide cyclase: The enzyme establishing the stereochemistry of octadecanoids and jasmonates. *J. Boil. Chem.* **2000**, *275*, 19132–19138. [[CrossRef](#)]
7. Wu, Q.; Wu, J.; Sun, H.; Zhang, D.; Yu, D. Sequence and expression divergence of the AOC gene family in soybean: Insights into functional diversity for stress responses. *Biotechnol. Lett.* **2011**, *33*, 1351–1359. [[CrossRef](#)]
8. Wang, Y.; Liu, H.; Xin, Q. Improvement of copper tolerance of *Arabidopsis* by transgenic expression of an allene oxide cyclase gene, *GhAOC1*, in upland cotton (*Gossypium hirsutum* L.). *Crop J.* **2015**, *3*, 343–352. [[CrossRef](#)]
9. Stenzel, I.; Hause, B.; Miersch, O.; Kurz, T.; Maucher, H.; Weichert, H.; Ziegler, J.; Feussner, I.; Wasternack, C. Jasmonate biosynthesis and the allene oxide cyclase family of *Arabidopsis thaliana*. *Plant Mol. Boil.* **2003**, *51*, 895–911. [[CrossRef](#)]
10. Zdyb, A.; Salgado, M.G.; Demchenko, K.N.; Brenner, W.G.; Płaszczycza, M.; Stumpe, M.; Herrfurth, C.; Feussner, I.; Pawlowski, K. Allene oxide synthase, allene oxide cyclase and jasmonic acid levels in *Lotus japonicus* nodules. *PLoS ONE* **2018**, *13*, e0190884. [[CrossRef](#)]
11. Neumann, P.; Brodhun, F.; Sauer, K.; Herrfurth, C.; Hamberg, M.; Brinkmann, J.; Scholz, J.; Dickmanns, A.; Feussner, I.; Ficner, R. Crystal structures of *Physcomitrella patens* AOC1 and AOC2: Insights into the enzyme mechanism and differences in substrate specificity. *Plant Physiol.* **2012**, *160*, 1251–1266. [[CrossRef](#)] [[PubMed](#)]
12. Riemann, M.; Haga, K.; Shimizu, T.; Okada, K.; Ando, S.; Mochizuki, S.; Nishizawa, Y.; Yamanouchi, U.; Nick, P.; Yano, M.; et al. Identification of rice *Allene Oxide Cyclase* mutants and the function of jasmonate for defence against *Magnaporthe oryzae*. *Plant J.* **2013**, *74*, 226–238. [[CrossRef](#)] [[PubMed](#)]
13. Maucher, H.; Stenzel, I.; Miersch, O.; Stein, N.; Prasad, M.; Zierold, U.; Schweizer, P.; Dorer, C.; Hause, B.; Wasternack, C. The allene oxide cyclase of barley (*Hordeum vulgare* L.)—cloning and organ-specific expression. *Phytochemistry* **2004**, *65*, 801–811. [[CrossRef](#)] [[PubMed](#)]
14. Pi, Y.; Liao, Z.; Jiang, K.; Huang, B.; Deng, Z.; Zhao, D.; Zeng, H.; Sun, X.; Tang, K. Molecular cloning, characterization and expression of a jasmonate biosynthetic pathway gene encoding allene oxide cyclase from *Camptotheca acuminata*. *Biosci. Rep.* **2008**, *28*, 349. [[CrossRef](#)]
15. Stenzel, I.; Otto, M.; Delker, C.; Kirmse, N.; Schmidt, D.; Miersch, O.; Hause, B.; Wasternack, C. *ALLENE OXIDE CYCLASE* (AOC) gene family members of *Arabidopsis thaliana*: Tissue- and organ-specific promoter activities and *in vivo* heteromerization. *J. Exp. Bot.* **2012**, *63*, 6125–6138. [[CrossRef](#)]
16. Isayenkov, S.; Mrosk, C.; Stenzel, I.; Strack, D.; Hause, B. Suppression of allene oxide cyclase in hairy roots of *Medicago truncatula* reduces jasmonate levels and the degree of Mycorrhization with *Glomus intraradices*. *Plant Physiol.* **2005**, *139*, 1401–1410. [[CrossRef](#)]
17. Zhao, Y.; Dong, W.; Zhang, N.; Ai, X.; Wang, M.; Huang, Z.; Xiao, L.; Xia, G. A wheat allene oxide cyclase gene enhances salinity tolerance via jasmonate signaling. *Plant Physiol.* **2014**, *164*, 1068–1076. [[CrossRef](#)]
18. Wu, Q.; Wang, H.; Wu, J.; Wang, D.; Wang, Y.; Zhang, L.; Huang, Z.; Yu, D. Soybean *GmAOC3* promotes plant resistance to the common cutworm by increasing the expression of genes involved in resistance and volatile substance emission in transgenic tobaccos. *J. Plant Boil.* **2015**, *58*, 242–251. [[CrossRef](#)]

19. Hazman, M.; Hause, B.; Eiche, E.; Nick, P.; Riemann, M. Increased tolerance to salt stress in OPDA-deficient rice *ALLENE OXIDE CYCLASE* mutants is linked to an increased ROS-scavenging activity. *J. Exp. Bot.* **2015**, *66*, 3339–3352. [[CrossRef](#)]
20. Guo, H.M.; Li, H.C.; Zhou, S.R.; Xue, H.W.; Miao, X.X. Cis-12-oxo-phytodienoic acid stimulates rice defense response to a piercing-sucking insect. *Mol. Plant* **2014**, *7*, 1683–1692. [[CrossRef](#)]
21. Liu, H.; Wang, Y.; Wang, S.; Li, H. Cloning and characterization of peanut allene oxide cyclase gene involved in salt-stressed responses. *Genet. Mol. Res.* **2015**, *14*, 2331–2340. [[CrossRef](#)] [[PubMed](#)]
22. Zhou, Y.; Chen, L.; Xu, Y.; Wang, Y.; Wang, S.; Ge, X. The *CfAOS* and *CfAOC* genes related to flower fragrance biosynthesis in *Cymbidium faberi* could confer drought tolerance to transgenic tomatoes. *Int. J. Agric. Biol.* **2018**, *20*, 883–892.
23. Yang, Y.X.; Wu, C.; Ahammed, G.J.; Wu, C.; Yang, Z.; Wan, C.; Chen, J. Red light-induced systemic resistance against root-knot nematode is mediated by a coordinated regulation of salicylic acid, jasmonic acid and redox signaling in watermelon. *Front. Plant Sci.* **2018**, *9*, 899. [[CrossRef](#)] [[PubMed](#)]
24. Yang, Y.X.; Wang, M.M.; Ren, Y.; Onac, E.; Zhou, G.; Peng, S.; Xia, X.J.; Shi, K.; Zhou, Y.H.; Yu, J.Q. Light-induced systemic resistance in tomato plants against root-knot nematode *Meloidogyne incognita*. *Plant Growth Regul.* **2015**, *76*, 167–175. [[CrossRef](#)]
25. Nahar, K.; Kyndt, T.; De Vleeschauwer, D.; Höfte, M.; Gheysen, G. The jasmonate pathway is a key player in systemically induced defense against root knot nematodes in rice. *Plant Physiol.* **2011**, *157*, 305–316. [[CrossRef](#)] [[PubMed](#)]
26. Zhao, W.; Zhou, X.; Lei, H.; Fan, J.; Yang, R.; Li, Z.; Hu, C.; Li, M.; Zhao, F.; Wang, S. Transcriptional evidence for cross talk between JA and ET or SA during root-knot nematode invasion in tomato. *Physiol. Genom.* **2018**, *50*, 197–207. [[CrossRef](#)] [[PubMed](#)]
27. Naor, N.; Gurung, F.B.; Ozalvo, R.; Bucki, P.; Sanadhya, P.; Miyara, S.B. Tight regulation of allene oxide synthase (AOS) and allene oxide cyclase-3 (AOC3) promote *Arabidopsis* susceptibility to the root-knot nematode *Meloidogyne javanica*. *Eur. J. Plant Pathol.* **2018**, *150*, 149–165. [[CrossRef](#)]
28. Zhou, Y.; Ge, L.; Li, G.; He, P.; Yang, Y.; Liu, S. In silico identification and expression analysis of Rare Cold Inducible 2 (RCI2) gene family in cucumber. *J. Plant Biochem. Biotechnol.* **2019**. [[CrossRef](#)]
29. Guo, S.; Zhang, J.; Sun, H.; Salse, J.; Lucas, W.J.; Zhang, H.; Zheng, Y.; Mao, L.; Ren, Y.; Wang, Z.; et al. The draft genome of watermelon (*Citrullus lanatus*) and resequencing of 20 diverse accessions. *Nat. Genet.* **2013**, *45*, 51–58. [[CrossRef](#)]
30. Zhou, Y.; Li, J.; Wang, J.; Yang, W.; Yang, Y. Identification and characterization of the glutathione peroxidase (GPX) gene family in watermelon and its expression under various abiotic stresses. *Agronomy* **2018**, *8*, 206. [[CrossRef](#)]
31. Jiang, K.; Liao, Z.; Pi, Y.; Huang, Z.; Hou, R.; Cao, Y.; Wang, Q.; Sun, X.; Tang, K. Molecular cloning and expression profile of a jasmonate biosynthetic pathway gene for allene oxide cyclase from *Hyoscyamus niger*. *Mol. Boil.* **2008**, *42*, 381–390. [[CrossRef](#)]
32. Liu, B.; Wang, W.; Gao, J.; Chen, F.; Wang, S.; Xu, Y.; Tang, L.; Jia, Y. Molecular cloning and characterization of a jasmonate biosynthetic pathway gene for allene oxide cyclase from *Jatropha curcas*. *Acta Physiol. Plant.* **2010**, *32*, 531–539. [[CrossRef](#)]
33. Lu, X.; Lin, X.; Shen, Q.; Zhang, F.; Wang, Y.; Chen, Y.; Wang, T.; Wu, S.; Tang, K. Characterization of the jasmonate biosynthetic gene allene oxide cyclase in *Artemisia annua* L., source of the antimalarial drug artemisinin. *Plant Mol. Biol. Rep.* **2011**, *29*, 489–497. [[CrossRef](#)]
34. Habora, M.E.E.; Eltayeb, A.E.; Oka, M.; Tsujimoto, H.; Tanaka, K. Cloning of allene oxide cyclase gene from *Leymus mollis* and analysis of its expression in wheat–*Leymus* chromosome addition lines. *Breed. Sci.* **2013**, *63*, 68–76. [[CrossRef](#)]
35. Wang, M.X.; Ma, Q.P.; Han, B.Y.; Li, X.H. Molecular cloning and expression of a jasmonate biosynthetic gene allene oxide cyclase from *Camellia sinensis*. *Can. J. Plant Sci.* **2016**, *96*, 109–116. [[CrossRef](#)]
36. Hofmann, E.; Zerbe, P.; Schaller, F. The crystal structure of *Arabidopsis thaliana* allene oxide cyclase: Insights into the oxylipin cyclization reaction. *Plant Cell* **2006**, *18*, 3201–3217. [[CrossRef](#)]
37. Gu, X.C.; Chen, J.F.; Xiao, Y.; Di, P.; Xuan, H.J.; Zhou, X.; Zhang, L.; Chen, W.S. Overexpression of allene oxide cyclase promoted tanshinone/phenolic acid production in *Salvia miltiorrhiza*. *Plant Cell Rep.* **2012**, *31*, 2247–2259. [[CrossRef](#)]

38. Martínez-Medina, A.; Fernández, I.; Lok, G.B.; Pozo, M.J.; Pieterse, C.M.; Van Wees, S.C. Shifting from priming of salicylic acid- to jasmonic acid-regulated defences by *Trichoderma* protects tomato against the root knot nematode *Meloidogyne incognita*. *New Phytol.* **2017**, *213*, 1363–1377. [[CrossRef](#)]
39. Cerrudo, I.; Keller, M.M.; Cargnel, M.D.; Demkura, P.V.; De Wit, M.; Patitucci, M.S.; Pierik, R.; Pieterse, C.M.; Ballaré, C.L. Low red/far-red ratios reduce Arabidopsis resistance to *Botrytis cinerea* and jasmonate responses via a COI1-JAZ10-dependent, salicylic acid-independent mechanism. *Plant Physiol.* **2012**, *158*, 2042–2052. [[CrossRef](#)]
40. Kazan, K.; Manners, J.M. The interplay between light and jasmonate signalling during defence and development. *J. Exp. Bot.* **2011**, *62*, 4087–4100. [[CrossRef](#)]
41. Thorpe, M.R.; Ferrieri, A.P.; Herth, M.M.; Ferrieri, R.A. 11C-imaging: Methyl jasmonate moves in both phloem and xylem, promotes transport of jasmonate, and of photoassimilate even after proton transport is decoupled. *Planta* **2007**, *226*, 541–551. [[CrossRef](#)] [[PubMed](#)]
42. Lacombe, B.; Achard, P. Long-distance transport of phytohormones through the plant vascular system. *Curr. Opin. Plant Boil.* **2016**, *34*, 1–8. [[CrossRef](#)] [[PubMed](#)]
43. Heil, M.; Ton, J. Long-distance signalling in plant defence. *Trends Plant Sci.* **2008**, *13*, 264–272. [[CrossRef](#)] [[PubMed](#)]



© 2019 by the authors. Licensee MDPI, Basel, Switzerland. This article is an open access article distributed under the terms and conditions of the Creative Commons Attribution (CC BY) license (<http://creativecommons.org/licenses/by/4.0/>).